

UC Santa Barbara

UC Santa Barbara Previously Published Works

Title

Wildfire Risk in the Complex Terrain of the Santa Barbara Wildland–Urban Interface during Extreme Winds

Permalink

<https://escholarship.org/uc/item/88j9288v>

Journal

Fire, 5(5)

ISSN

2571-6255

Authors

Zigner, Katelyn
Carvalho, Leila MV
Jones, Charles
et al.

Publication Date

2022





DOI

10.3390/fire5050138

Peer reviewed

Article

Wildfire Risk in the Complex Terrain of the Santa Barbara Wildland–Urban Interface during Extreme Winds

Katelyn Zigner ^{1,*}, Leila M. V. Carvalho ^{1,2} , Charles Jones ^{1,2} , John Benoit ³, Gert-Jan Duine ² , Dar Roberts ^{1,2} , Francis Fujioka ⁴, Max Moritz ^{1,2,5}, Nic Elmquist ⁶ and Rob Hazard ⁷

¹ Department of Geography, University of California, Santa Barbara, CA 93106, USA

² Earth Research Institute, Santa Barbara, CA 93106, USA

³ U.S. Forest Service, Pacific Southwest Research Station, Riverside, CA 92507, USA

⁴ Institute for Earth, Computing, Human and Observing, Chapman University, Orange, CA 92866, USA

⁵ University of California Cooperative Extension, Santa Barbara, CA 93106, USA

⁶ Montecito Fire Department, Santa Barbara, CA 93108, USA

⁷ Santa Barbara County Fire Department, Santa Barbara, CA 93110, USA

* Correspondence: katelyn.zigner@noaa.gov

Abstract: Each year, wildfires ravage the western U.S. and change the lives of millions of inhabitants. Situated in southern California, coastal Santa Barbara has witnessed devastating wildfires in the past decade, with nearly all ignitions started by humans. Therefore, estimating the risk imposed by unplanned ignitions in this fire-prone region will further increase resilience toward wildfires. Currently, a fire-risk map does not exist in this region. The main objective of this study is to provide a spatial analysis of regions at high risk of fast wildfire spread, particularly in the first two hours, considering varying scenarios of ignition locations and atmospheric conditions. To achieve this goal, multiple wildfire simulations were conducted using the FARSITE fire spread model with three ignition modeling methods and three wind scenarios. The first ignition method considers ignitions randomly distributed in 500 m buffers around previously observed ignition sites. Since these ignitions are mainly clustered around roads and trails, the second method considers a 50 m buffer around this built infrastructure, with ignition points randomly sampled from within this buffer. The third method assumes a Euclidean distance decay of ignition probability around roads and trails up to 1000 m, where the probability of selection linearly decreases further from the transportation paths. The ignition modeling methods were then employed in wildfire simulations with varying wind scenarios representing the climatological wind pattern and strong, downslope wind events. A large number of modeled ignitions were located near the major-exit highway running north–south (HWY 154), resulting in more simulated wildfires burning in that region. This could impact evacuation route planning and resource allocation under climatological wind conditions. The simulated fire areas were smaller, and the wildfires did not spread far from the ignition locations. In contrast, wildfires ignited during strong, northerly winds quickly spread into the wildland–urban interface (WUI) toward suburban and urban areas.

Keywords: wildfire modeling; FARSITE; fire weather; Sundowner winds; ignition modeling; WUI



Citation: Zigner, K.; Carvalho, L.M.V.; Jones, C.; Benoit, J.; Duine, G.-J.; Roberts, D.; Fujioka, F.; Moritz, M.; Elmquist, N.; Hazard, R. Wildfire Risk in the Complex Terrain of the Santa Barbara Wildland–Urban Interface during Extreme Winds. *Fire* **2022**, *5*, 138. <https://doi.org/10.3390/fire5050138>

Academic Editor: Alan F. Talhelm

Received: 19 August 2022

Accepted: 14 September 2022

Published: 18 September 2022

Publisher's Note: MDPI stays neutral with regard to jurisdictional claims in published maps and institutional affiliations.



Copyright: © 2022 by the authors. Licensee MDPI, Basel, Switzerland. This article is an open access article distributed under the terms and conditions of the Creative Commons Attribution (CC BY) license (<https://creativecommons.org/licenses/by/4.0/>).

1. Introduction

Destructive wildfires in the western U.S., and especially in California, occur every year, greatly impacting the lives of millions of inhabitants. Some of the most impactful wildfires occur in the rapidly-growing wildland–urban interface (WUI), which is the area where communities are intermixed with the surrounding natural environment [1–3]. More specifically, regions may be divided into smaller classes such as urban, WUI interface, WUI intermix, and rural [4,5]. The majority of fatalities, home losses, and fire suppression costs occur in the WUI under critical weather conditions [4], and WUI expansion has increased the probability of ignition and the general wildfire risk [6–9]. Further complicated

by complex and mountainous terrain, this is true for the WUI in coastal Santa Barbara, CA, USA.

Most wildfires are started by humans in southern California [10], and in Santa Barbara County approximately 99% of historical wildfire ignitions are due to humans [11]. Human expansion into rural areas leads to greater housing developments and increased wildfire risk [2,12,13]. Human-ignited fires occur year-round [14], and those occurring in the absence of strong winds are relatively easy to control and contain [15]. Additionally, human-ignited wildfires account for 84% of all wildfires ignited and 44% of the area burned in the U.S. [10]. Ignition patterns in southern California are related to distance to roads, trails, and human development, as well as slope and fuel type [8,16,17]. In fact, the distance to road explained about 40% of the ignitions in the Santa Monica Mountains and San Diego County [18]. Maximum fire frequency occurs in areas with an intermediate level of human activity, though the area burned is less related to this factor [7]. Areas with a high probability of ignition and that are prone to extreme winds are of greatest fire risk and attention [18].

Three factors, known as the ‘fire triangle’, control fire behavior [19]: fuels, topography, and weather. Other factors that may influence fire spread include live fuel moisture, burn scars from previous fires, and preventative fire measures such as fuel treatments. However, during critical fire weather conditions, wind is the dominant factor in determining fire spread [20,21]. In coastal Santa Barbara County, the most critical fire weather is often associated with downslope windstorms on the slopes of the Santa Ynez Mountains (SYM), known as Sundowner winds or Sundowners [22–24]. Sundowners occur year-round [23] and may create critical fire weather conditions as the strong, northerly dry winds rapidly spread fires southward toward highly populated areas (Figure 1a) [25–29]. Sundowners have enhanced fire spread in all seasons, particularly in the summer and fall, when strong winds and dry fuels enhance large, impactful wildfires [25,29,30]. In fact, more hectares are burned during extreme wind conditions than non-extreme wind conditions [31].

Although a decrease in relative humidity and temperature increases are case-dependent [22,24,26], Sundowners often create critical fire weather conditions due to gusty winds and a lowered dew point [25,30]. The strongest winds are observed along the middle of the SYM mountain slopes, though strong winds may extend into the foothills and onto the coastal plain [23,24,26,27]. One study [23] utilized a combined empirical orthogonal function analysis on the zonal and meridional winds from a 30-year Weather Research and Forecasting (WRF) model simulation at 1 km grid resolution [32]. The study found existence of three Sundowner regimes: Western, Eastern, and Santa Barbara (a combination of Western and Eastern). The majority of coastal Santa Barbara inhabitants live in a region that is often affected by the “Eastern” or “Santa Barbara” Sundowner, with winds typically exhibiting a north-to-northeast direction. Furthermore, few major roads serve the relatively dense population living in the foothills and urban centers. The main east–west road running through coastal Santa Barbara is HWY 101, and the only route heading north from the city of Santa Barbara is HWY 154 (Figures 1a and A1), which has been closed due to multiple wildfires in the past. Another important road is Cathedral Oaks Road (labeled “CO” in Figure 1a), which is the only road that allows access to and from homes in the foothills north of the cities. Some of these wildfires have crossed these major routes, such as the Painted Cave (1990), Tea (2008), Jesusita (2009), Sherpa (2016), Thomas (2017), Cave (2019), and Alisal (2021; not shown) fires have come close (Figure 1a).

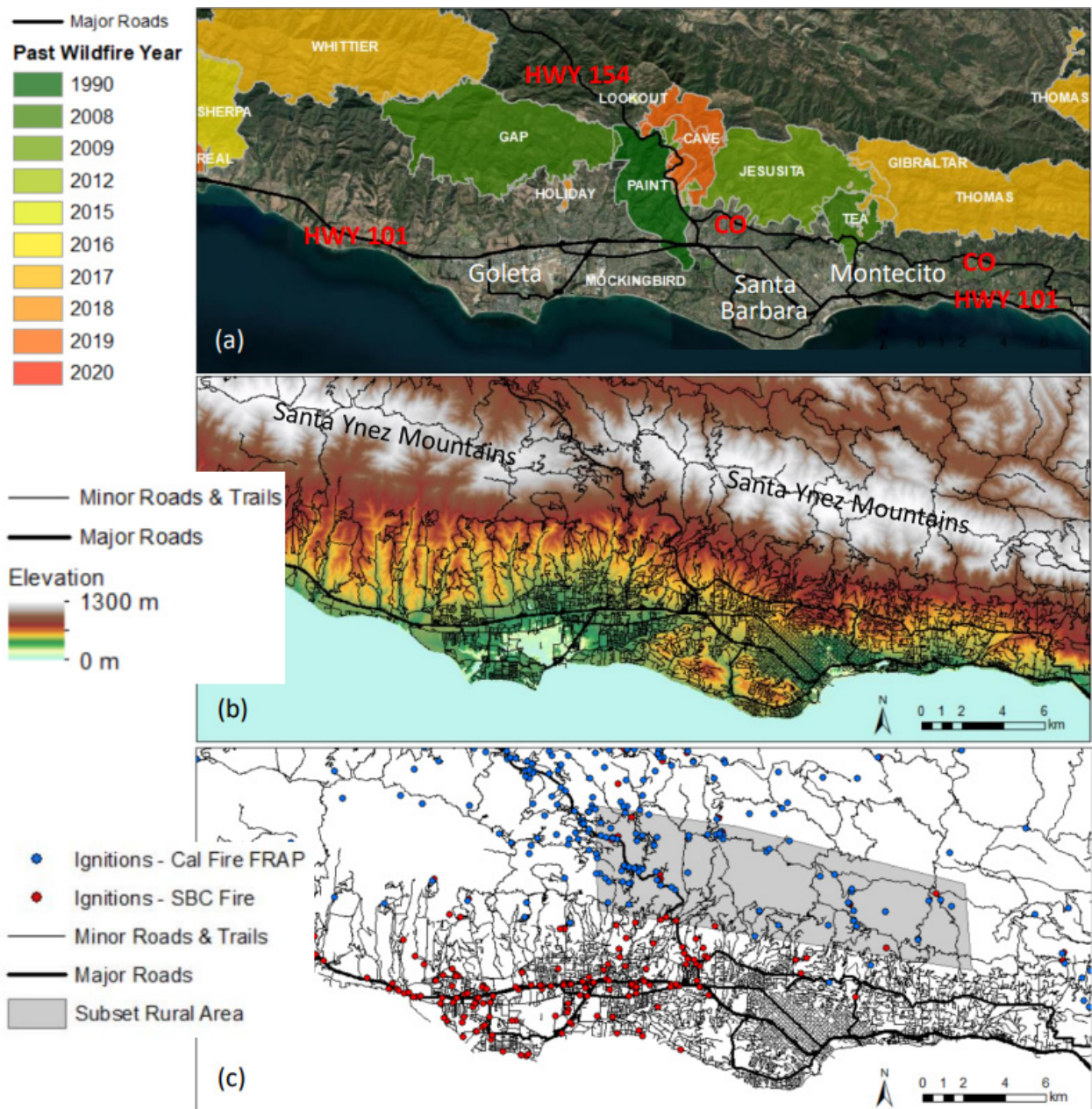


Figure 1. Study area. (a) Satellite imagery overlaid with previous wildfires (colored polygons), and major roads (thick, black lines and uppercase red text). The label “CO” stands for “Cathedral Oaks Road”. The names of previous wildfire are smaller and in uppercase text, and cities are in larger, sentence-case text. (b) Terrain elevation (colored) and important roads and trails. Major roads are shown as thick lines and minor roads are shown as thinner lines. (c) Roads and trails (lines) with previous ignitions overlaid. Color indicates the ignition source database. The area subset for ignition modeling to the north of the cities is shaded gray. A reference map showing the location of Santa Barbara and this coastal subset can be found in Figure A1.

Pre-fire planning is necessary for an effective response to fire and to mitigate potential future wildfires [33]. The first couple of hours after ignition are the most important in terms of evacuation enforcement, particularly in the WUI and in urban areas. Multiple ideas have been proposed to increase resilience to wildfires. Land use planning and fuel treatments may be used to create a buffer zone around the WUI [6]. However, it is important to note that lower fuel loads resulting from fuel treatments will not stop wildfires during extreme fire weather, but the fire intensity would likely decrease and allow for methodical fire

suppression techniques [6,34]. Although wildfire suppression via methods such as fuel treatments are relatively effective (95–98%) [35], this may lead to large and destructive wildfires that are difficult to suppress [36,37]. Furthermore, wildfire risk may be decreased by reducing the potential for building ignition, but this requires action by homeowners and private landowners rather than via an agency [35,38,39]. Another method is to bury power lines [31], since many California wildfires are ignited by electrical above-ground powerline failures or the falling of powerlines. Finally, staged resources and additional staffing on critical weather days can increase fire resilience in the event of an ignition [31]. When the Holiday Fire ignited in the foothills of Goleta in July 2018 [29], resources had been strategically placed and additional staff were prepared [29]. The fire was quickly contained, and damages and costs were minimized on a critical weather day that could have ended in disaster.

Fire spread models such as the FARSITE fire area simulator [40] are commonly used operationally to determine wildfire size, location, and timing in operations for wildfire incidents [41–44]. This is an uncoupled model, meaning that the interactions between the fire and the microscale meteorology at the fire front are not interacting. FARSITE uses Huygen's principle of wave propagation and the Rothermel fire spread equations to propagate fires using elliptical shapes at vertices on the fire front based on fuels, topography, and wind [45]. The primary limitation of this model is the lack of interaction between the fire and the microscale weather, particularly at the fire front, where this feedback can influence fire spread and intensity. The advantages of FARSITE include a low computational expense and relatively quick runtime, which can be essential in emergency situations. Additional limitations and advantages of this model and more can be found in [44]. The authors of [30] used FARSITE to simulate two significant wildfires in the region: the Sherpa (June 2016) and Painted Cave (1990) fires. They found that FARSITE could simulate wildfires that had a small amount of spotting, or the phenomena of embers carried by the wind to a new location typically ahead of the fire front, fairly well (i.e., the Sherpa fire). However, the spotting algorithm in FARSITE does not allow for spotting during downslope fire spread and thus underestimated the burned area of fires that had large amounts of spotting (i.e., the Painted Cave fire). Despite this limitation, the study demonstrated the utility of simple, uncoupled models like FARSITE in simulating the general behavior of wildfires on the SYM slopes in the first 1–2 h after ignition, which is useful for the purposes of fast and efficient evacuation.

A handful of previous studies have analyzed fire risk by creating wildfire maps using statistical models [9,46–49]. However, no studies have focused on local scales (<1 km grid spacing for fuels and weather), and none have studied Sundowners specifically. The primary goal of this study is to identify areas at the highest wildfire risk under various ignition modeling methods and wind scenarios in the fire-prone coastal Santa Barbara region. Given that the majority of wildfires are ignited by humans in Santa Barbara, the following specific questions are investigated: how do the simulated wildfire spread frequency and rate of spread vary with respect to previously observed ignitions and distance to roads and trails? What are the areas at highest risk in Santa Barbara during non-Sundowner conditions and during Sundowner conditions? To answer these questions, we examine three methods of wildfire ignition modeling and perform FARSITE simulations with distinct initial conditions for wind input. Wildfire risk maps are assessed based on the frequency of burned areas and minimum time of arrival of the wildfires under various ignition and wind conditions. The paper is organized as follows: Section 2 explains the data and methods, and Section 3 investigates differences in ignition modeling methods and the resulting variability in risk maps with varying ignition locations and wind scenarios. The discussion and conclusions are provided in Section 4.

2. Data and Methods

2.1. Study Area

Situated on the California coast between Los Angeles and San Francisco, picturesque coastal Santa Barbara County is located between the Santa Barbara Channel (part of the Pacific Ocean) to the south and the east–west oriented Santa Ynez Mountains to the north (Figures 1b and A1). Spanning approximately 100 km, the Santa Ynez Mountains (SYM) exhibit a width around 10 km and peaks around 1.2 km, with a generally decreasing ridgeline height toward the west. The numerous canyons on the south side of the mountains channel winds, creating localized gusty areas and increasing fire danger especially during Sundowners.

From west to east, the populated cities in coastal Santa Barbara include Goleta, Santa Barbara, and Montecito, totaling approximately 150,000 people. Many inhabitants live in the SYM foothills or on the mountains, generally within or near the WUI [50]. Few narrow and winding roads serve these regions, increasing danger in this wildfire-prone region (Figure 1).

2.2. Road and Trail, Ignition, and Historical Wildfire Data

For a complete wildfire ignition modeling strategy that includes mainly human-caused ignitions, both transportation and ignition data are required. Vectorized road and trail data were provided from the U.S. Forest Service with the feature class subtype indicated for each segment, allowing for differentiation between major roads, minor roads, and trails (Figure 1b,c) (<https://data.fs.usda.gov/geodata/edw/datasets.php>; accessed on 12 August 2020).

Ignition data were pulled from two databases and span more than 30 years (1986–2019). The first ignition data source is the Santa Barbara County (SBC) Fire Department, which recorded ignitions in Santa Barbara County outside of the Los Padres National Forest (north of the city) from 2007 (data acquired upon request). Until 2016, the U.S. Forest Service (USFS) was not required to report ignitions to the county fire department, hence there is a likely undercount for ignitions in rural locations (Figure 1c) [51]. This ignition database ends in 2019 when it was requested by the authors. The second source of ignition data is from the U.S. Forest Service FIRESTAT fire Occurrence database and extends from 1986–2019 (<https://data.fs.usda.gov/geodata/edw/datasets.php>; accessed on 12 August 2020). All ignition points are located within the Los Padres National Forest, filling in the gaps from the SB County dataset (Figure 1c). In both datasets, each ignition point contains data on the ignition date and time, cause, location, containment date and time, incident number, agency, and number of acres burned. Although duplicate ignition points were not found within either database, we did determine some duplicates between the two datasets, as determined by matching coordinates and dates. When this occurred, only one data point was used in the statistical analysis. Wildfire perimeter data were pulled from the State of California Fire and Resource Assessment Program (FRAP) fire history database in shapefile format (<https://frap.fire.ca.gov/frap-projects/fire-perimeters>; accessed on 15 May 2020).

2.3. Ignition Modeling Methods

Three methods were used for modeling ignitions in the WUI and in wildland parts of the SYM slopes and foothills above the city of Santa Barbara and Montecito (see gray box in Figure 1c). This region was selected because of the increased risk that wildfires may rapidly spread toward highly populated regions during Sundowner winds. Between the SBC Fire dataset (2007–2019) and FIRESTAT dataset (1986–2019) described in the previous section, eighty-five ignition points have been reported in this area, including the ignition locations of devastating wildfires influenced by Sundowner winds such as the Painted Cave (1990), Tea (2008), Jesusita (2009), and Cave (2019) fires.

We specified 100 ignition sites for each of the three different methods. In the first ignition modeling method, 500 m buffers were created around previous ignition locations, and 100 new ignition points were randomly sampled from within these buffers (Figure 2a).

Since ignitions tend to be clustered around roads and trails, the second method used buffers of 50 m around this infrastructure with 100 ignition points randomly sampled from within this buffer (Figure 2b). The third method assumed a Euclidean distance decay around roads and trails up to 1000 m, where the probability of selection linearly decreased further from the transportation paths (Figure 2c). One-hundred new ignition points were then quasi-randomly sampled using the spatial weights. A similar method using a linear piecewise function was utilized in [47], where the probability of selection from 0–100 m from a roadbed was 1 and probability decreased to 0.1 at a distance of 1 km.

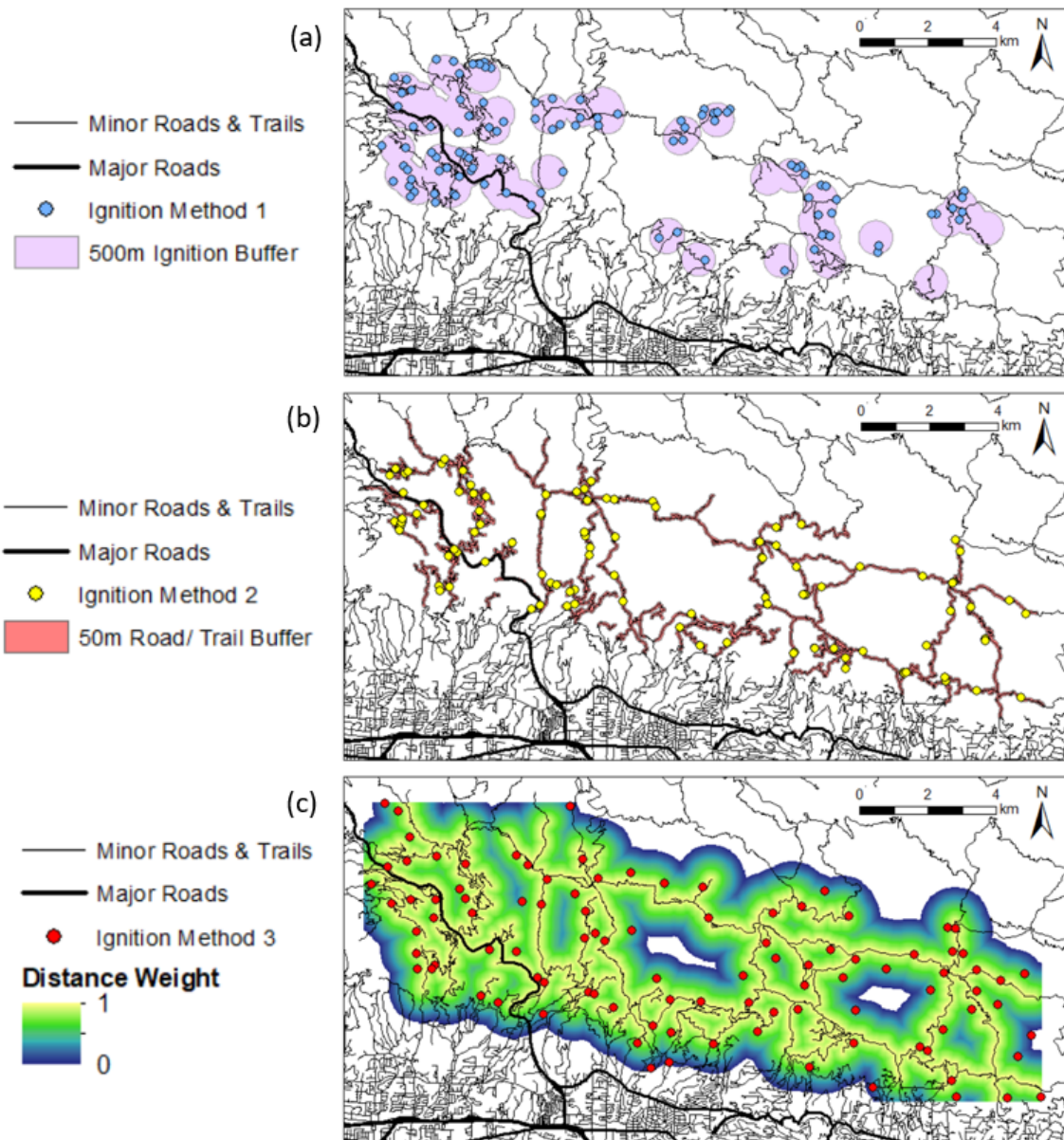


Figure 2. Results of the three ignition modeling methods overlaid on major (thick lines) and minor (thin lines) roads and trails. (a) Ignition modeling method 1: 500 m buffer (purple polygons) around previous ignition points with the modeled ignition points (blue dots). (b) Ignition modeling method 2: 50 m buffer (pink polygon) around roads and trails with the modeled ignition points (yellow dots). (c) Ignition modeling method 3: Distance–weight up to 1 km (colored) from roads and trails with modeled ignition points (red dots).

2.4. FARSITE and Model Input

To determine areas at high wildfire risk, simulations were performed using the FARSITE fire spread model [40] to create wildfire risk maps. The spotting algorithm was disabled due to limitations in simulating realistic wildfires during downslope windstorms [30]. Despite the spotting limitation and the lack of fire–atmosphere feedback interactions (as explained in the introduction), FARSITE was chosen for this study because of the low computational cost and relatively fast simulation runtimes which allowed for the running of hundreds of simulations. The fuel map was created by applying canonical discriminant analysis and linear discriminant analysis imagery from 2004 with 12 m spatial resolution from the Airborne Visible/Infrared Imaging Spectrometer (AVIRIS) [52]. This imagery was selected because of the high resolution and the lack of burn scars, which may be considered an unburnable fuel. The classified imagery was cross-walked into six fuel models: short grass, coastal sage scrub, shrubs, dense shrubs, trees/riparian, suburban/WUI, and urban/unburnable (Figure A2) (see [30] for fuel model details). Live fuel moistures were kept consistent in all simulations and were set as the values estimated for the 1990 Painted Cave fire. This was because southern California had been in a drought for years prior and some of the lowest fuel moistures in this region were recorded in 1990 [30].

To create wildfire risk maps, we performed numerous simulations using FARSITE with gridded wind data for three scenarios: non-Sundowner conditions, Sundowner conditions, and a Sundowner case study, chosen to represent a case with extreme winds (Figure 3). In our study, gridded composite (mean) wind rasters during non-Sundowner (climatological) and Sundowner conditions, defined as the Eastern Sundowner regime in [23], were calculated and created for use in FARSITE (Figure 3a,b). During the Eastern Sundowner regime, downslope winds (with predominant north-northeast direction) are typically stronger over the eastern portion of the SYM and affect populated areas in Santa Barbara and Montecito. Wildfires such as the Jesusita and Tea fires rapidly spread during significant Eastern Sundowner regimes [23]. Since composites smooth the strongest winds, we chose to also use winds from a Sundowner case study with winds exceeding 13 m/s (or 30 mph) at many grid cells in Goleta, Santa Barbara, and Montecito on 14 April 2005 (Figure 3c). To better compare the differences due to winds solely, all other atmospheric variables utilized in FARSITE (e.g., temperature and relative humidity for fuel drying purposes) were maintained constant among simulations and are the same as modeled at the ignition point of the 1990 Painted Cave fire on June 27. Details can be found in [30].

Wildfire risk maps were created for the three ignition modeling methods and the three gridded wind scenarios. Fires were ignited at every ignition point for the respective method. The ignition time was set to 2000 PST, aligning with typical Sundowner onset in the central and eastern parts of the SYM [23]. Fires were simulated using FARSITE for three hours after ignition.

3. Impacts of Varied Ignition Modeling Methods on Wildfire Spread

3.1. Ignitions in the WUI: Observations and Modeling

Generally, the observed ignitions are not uniform throughout the area of study. Rather, they are clustered in the eastern and western parts of the area of interest, around roads and trails on the SYM slopes and foothills (Figure A3). Therefore, the absence of ignitions in the middle of the area of interest in ignition methods 1 and 2 is explained by the lack of previously observed ignitions, and the distribution of roads and trails that were used in the modeling. Modeled ignitions are more dispersed in method 3, resulting in more ignitions to the north (toward the SYM ridgeline) and south (in the WUI and near the city). It is important to note that many ignitions surround HWY 154 (Figures 2 and A3), which serves as an important evacuation route for the community. This has implications for resource planning and allocation, in addition to evacuation planning [50].

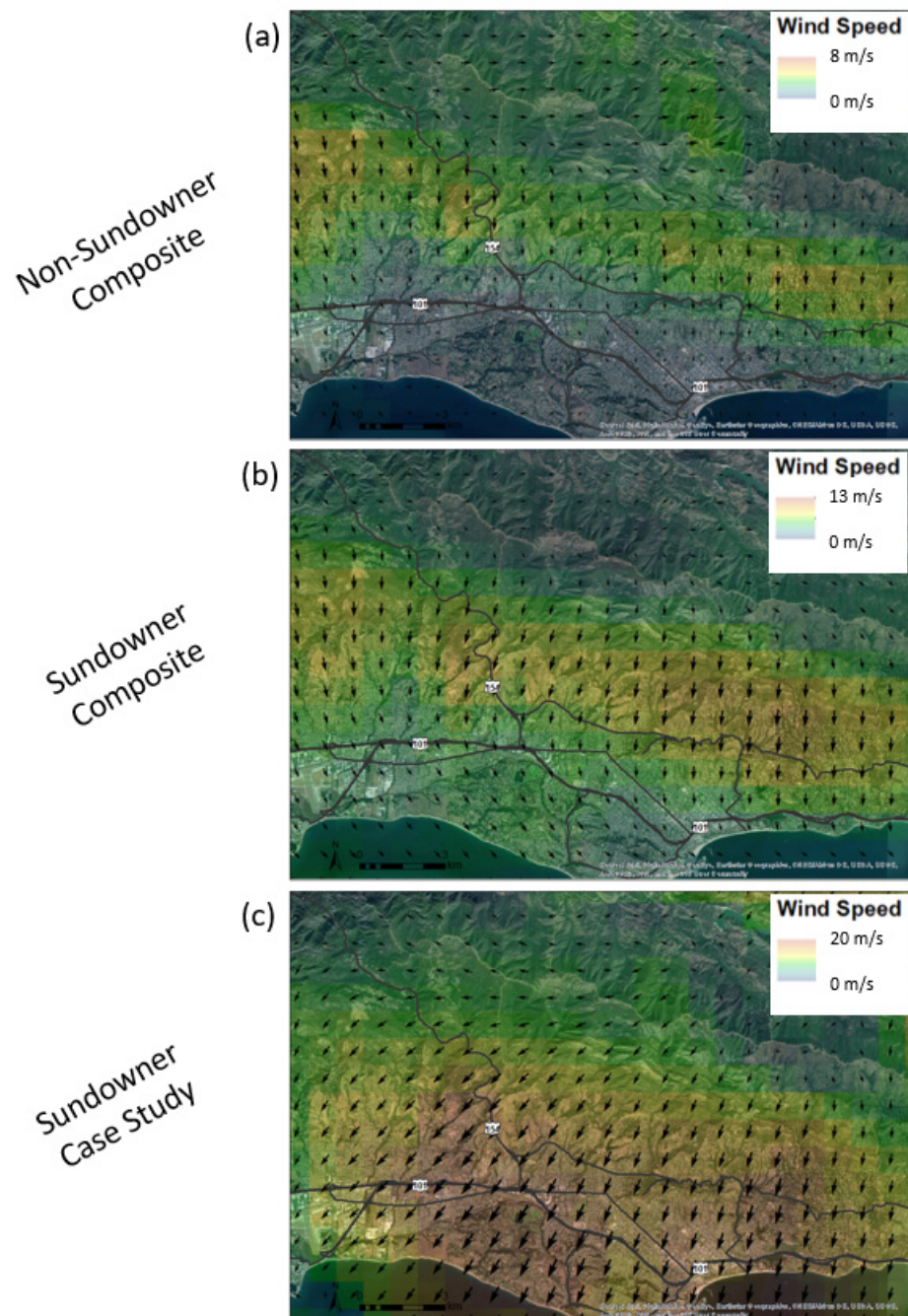


Figure 3. Gridded wind rasters using WRF data for (a) non-Sundowner composite, (b) Sundowner composite, and (c) Sundowner case study at 20 PST on 14 April 2005.

Figure 4 further illustrates the differences among methods by showing the distribution of distances between modeled ignitions with respect to the nearest observed ignition (Figure 4a), as well as the distances between ignitions and roads and trails (Figure 4b). As expected, the modeled ignitions in method 1 are the closest to the observed ignition locations. Nonetheless, the modal value of distance is between 200–300 m and very few are less than 100 m away (Figure 4a). The observed ignitions are farthest from the modeled ones in ignition method 3, which is explained by the larger expanse of potential ignition locations allowed by the method (Figure 2c). Concerning the distance between ignitions and the nearest road or trail, the observed ignitions are generally within 100 m of a road or trail, but there are a few that are over 500 m away (Figure 4b). Ignition methods 1 and 3 appear similar, with between 10–25% of the ignitions with distances between 0–300 m from

roads and trails, and less than 10% of ignitions with distances exceeding 300 m. In contrast, due to the constraints placed on ignition modeling method 2 (50 m buffer around roads and trails), all ignitions in that method are much closer and within a 50 m distance.

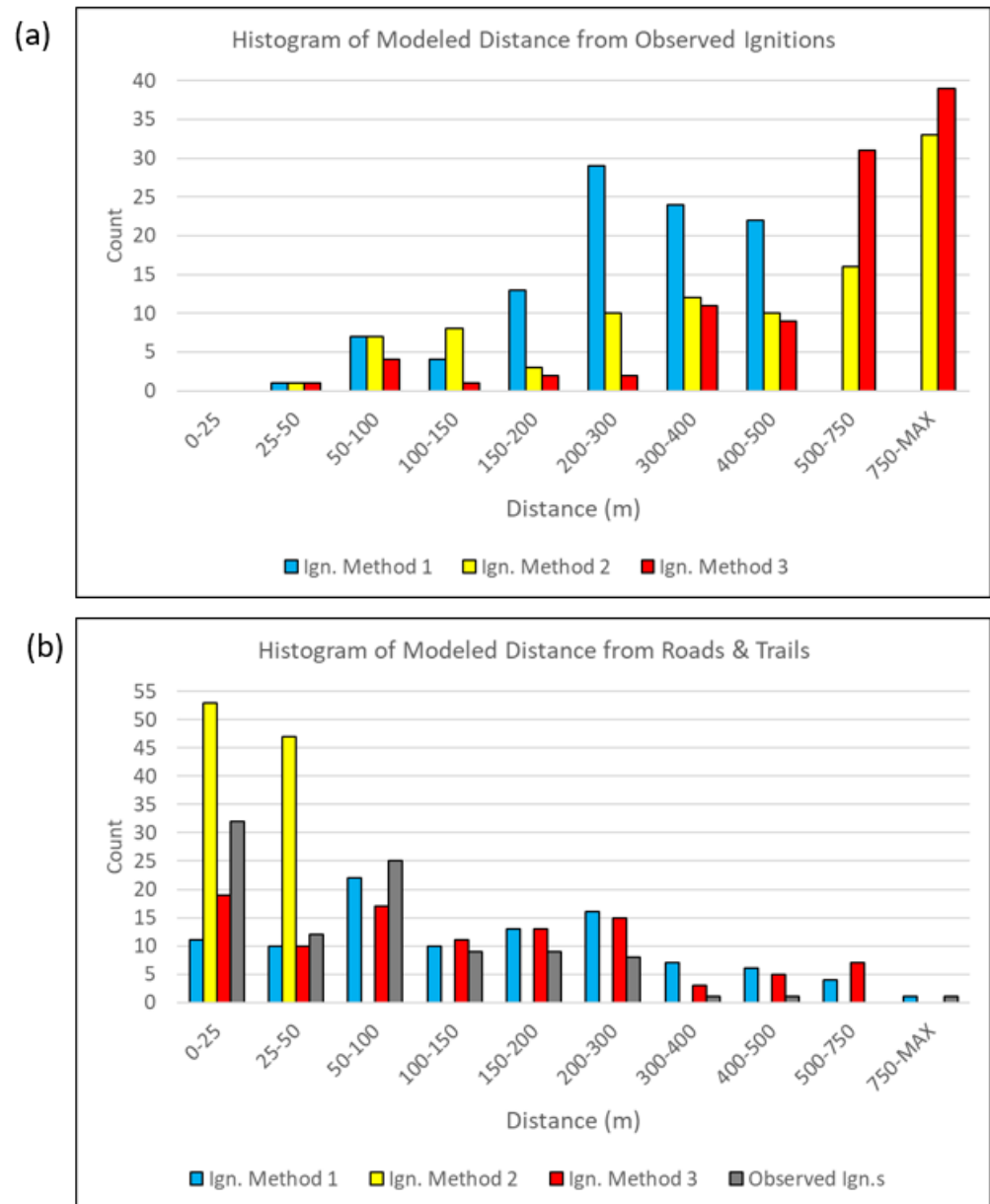


Figure 4. Bar plots showing the distance of each modeled ignition to the nearest observed ignition (a) and road or trail (b). The observed ignition distance to the nearest road or trail is included in (b). The total count for each method is 100.

3.2. Wildfire Spread Risk in the WUI using Varied Ignition Methods and Wind Scenarios

Here we assess the wildfire risk in the WUI of Santa Barbara using the three proposed ignition methods, focusing on two main aspects: (1) the spatial pattern of ‘hits’, or areas that have been hit by a simulated wildfire within the first three hours of simulations; and (2) the time of arrival (TOA) of a wildfire. The analysis of TOA is a metric to evaluate the rapid spread of a wildfire given the ignition point, the set of meteorological and fuel conditions, and the topography.

3.2.1. Climatological (Non-Sundowner) Conditions

First, we examine differences in ignition methods with mean winds simulated during non-Sundowner conditions (as defined in Section 2.4) during all seasons (Figure 5). Relatively weak winds less than 5 m/s were present throughout most of the domain (Figure 3a). For ignition method 1 (buffer around observed ignition locations), some areas near HWY 154 were hit by over 10 simulations and many areas were hit by at least four simulations, partially resulting from the cluster of ignitions in this region (Figure 5a). Multiple previous wildfires have occurred in this area (Figure 1a), putting this location at high risk of being hit by a wildfire. Two other relatively smaller areas in the eastern part of the region of interest were hit up to six times, and very few simulations hit areas in the middle. Results were similar for ignition method 2 (buffer around roads and trails); a few areas in the west and east had over six hits (Figure 5c). The simulated fires in ignition method 3 covered the most area of all ignition methods because of the greater dispersion of the ignitions compared to the other two methods. Therefore, this method represents a more spatially random approach to ignitions, while typically maintaining a close distance to roads and trails. Few grid cells were hit by more than five simulations, although more areas had at least 1 hit (Figure 5e).

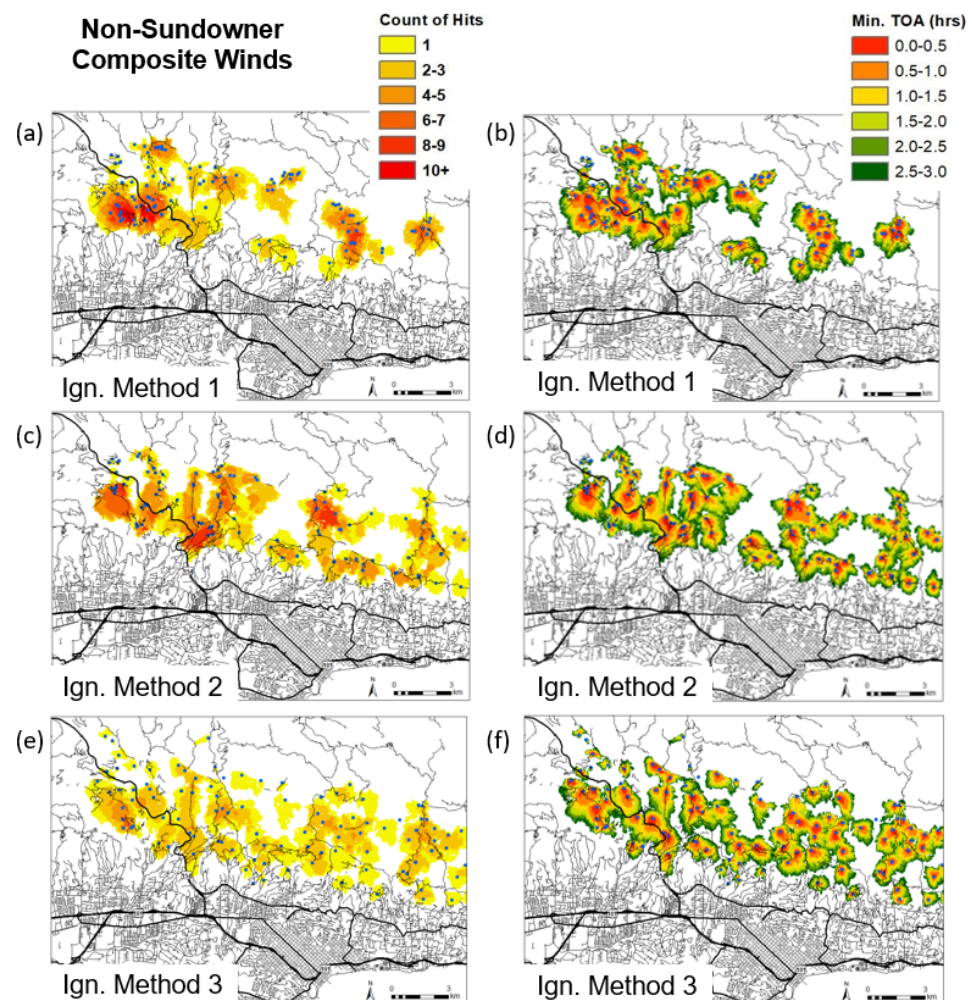


Figure 5. Maps showing the total number of hits by the 100 simulations at each grid cell (a,c,e) and the earliest time of arrival (TOA) at each grid cell in any of the simulations (b,d,f). Simulations were run using the non-Sundowner composite. Maps (a,b) show results from ignition method 1, (c,d) show results from ignition method 2, and (e,f) show results from ignition method 3. The lines are roads and trails, and the blue dots indicate the ignition locations for the specified ignition modeling method.

When considering all 300 simulations that used the climatological winds, regardless of ignition method, an area in the western part of the region of interest and to the west of HWY 154 was hit the most, by up to 25 simulations (~8% of all simulations) (Figure 6a). Multiple areas around HWY 154 and some areas in the west part of the region were hit by at least 13 (~4%) of the simulations. It's important to note that none of these simulations reached the evacuation route Cathedral Oaks Road and few spread into the WUI, explained by the absence of strong winds steering the fires in a particular direction.

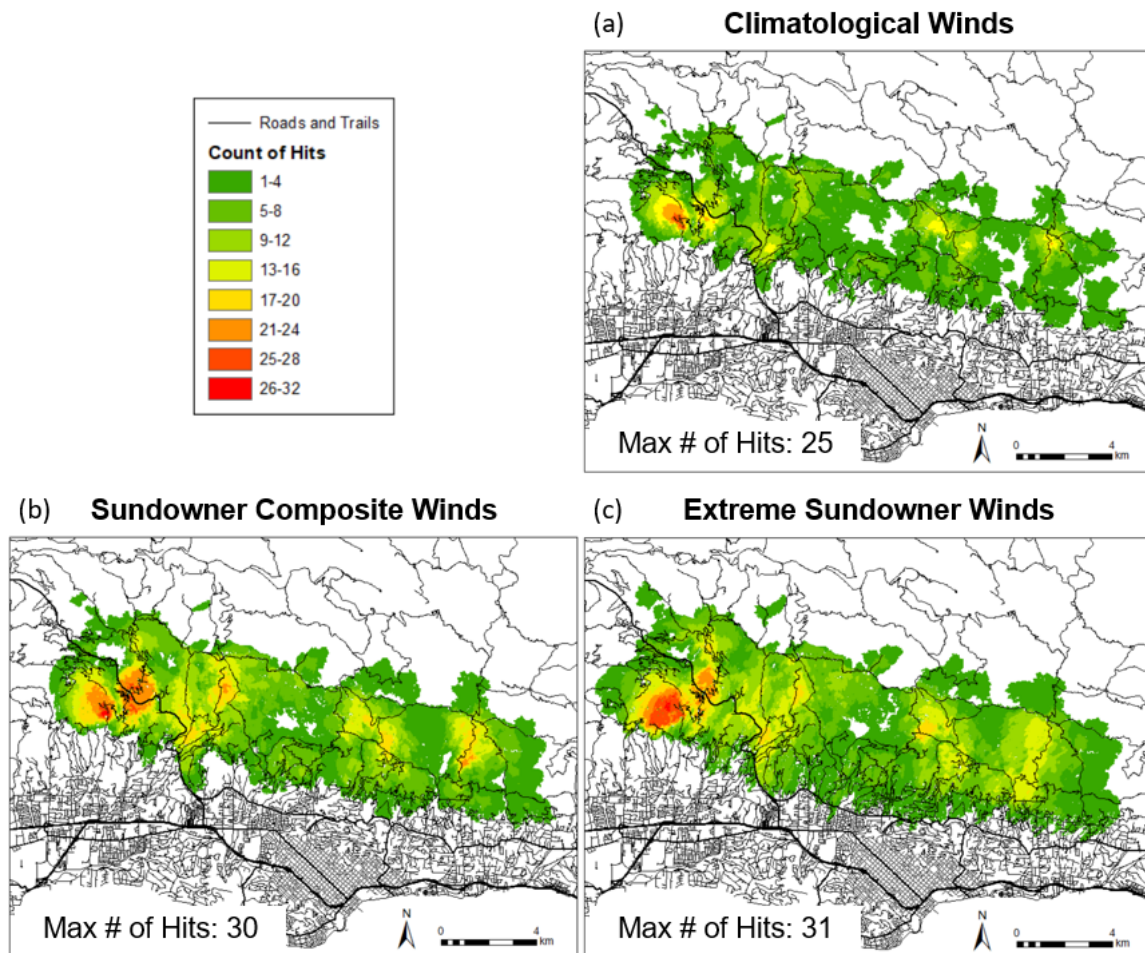


Figure 6. Similar to the subplots in Figure 5 showing the total number of hits at each grid cell, but all ignition methods were combined for (a) climatological wind input, (b) Sundowner composite wind input, and (c) extreme Sundowner case study wind input.

The simulated fires generally did not travel far from the ignition location and spread radially (Figure 5), given the relatively weak winds (<5 m/s) throughout the domain (Figure 3a). These results imply that during climatological mean wind conditions, fires are less likely to spread quickly toward highly populated areas to the south, assuming that temperatures, relative humidity, fuels, and fuel moistures are comparable.

Boxplots of simulated wildfire sizes separated by the meteorological condition and ignition method at half-hour intervals (from 0.5 h to 3 h after ignition) are shown in Figure 7. Simulated fires were the smallest during climatological conditions, usually growing to less than 30 ha in the first hour and less than 200 ha three hours after ignition (three left boxplots in Figure 7b,f). The largest wildfires were around 300 ha three hours after ignition. Notice that some wildfires were close to 0 ha due to unburnable fuels near the ignition location, which extinguished the fire early after ignition.

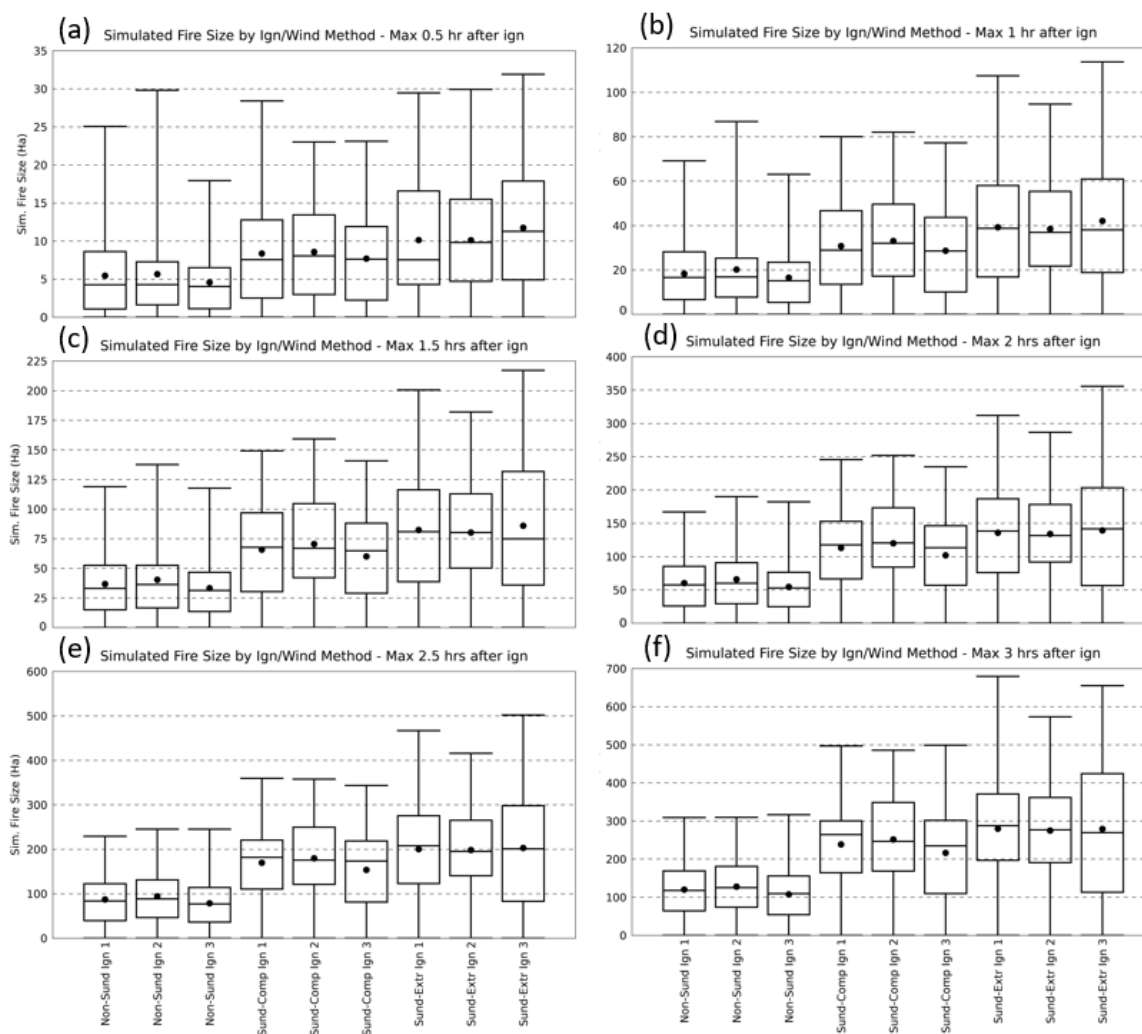


Figure 7. Boxplots showing the distribution of wildfire sizes for each ignition method and wind scenario combination every half hour. The whiskers identify the minimum and maximum values, and the box includes the lower quartile, median, and upper quartile. No outliers were identified, and the dot indicates the mean. Note the different y-axis values on each histogram.

Figure 8 shows the percentage of the total number of grid cells burned in the region of interest (columns) separated according to the number of times a simulation hit a cell in that domain (“# of Hits”, rows) for each ignition method and wind scenario analyzed in this study. Notice that the sum of each column is ~100% since only grid cells that were hit by at least one simulation for each ignition method and wind scenario combination were used in these statistics. For instance, during non-Sundowner conditions, simulations indicate that approximately 73%, 81% and 95% of the cells hit in at least 1 of the 100 simulations were hit between 1–3 times for ignition methods 1, 2, and 3, respectively. This means that method 1, which considers buffers around previous ignitions (probability of ignitions is highly non-uniform in the area, see Figures 1c and 2a), resulted in a relatively higher fraction of grid points that were hit more than six times, compared to the other two methods. In particular, the proximity of ignitions to HWY 154 in method 1 resulted in ~1.5% of grid cells being hit more than 10 times (Figure 8), whereas ignition methods 2 and 3 had no grid cells hit more than seven times. Conversely, ignition method 3 assumes the most dispersed ignition locations, and about 56% of the grid cells were only hit once. Although the number of hits should change with the number of simulations, the relative percentage of hits separated according to the ignition methods should follow a similar pattern. Since methods 1 and 2 have high weight on the previously observed sites of ignitions, these results indicate that

the probability of burn is not homogeneous in the region, and there are areas of relatively high risk of being hit by a wildfire, even during relatively calm winds.

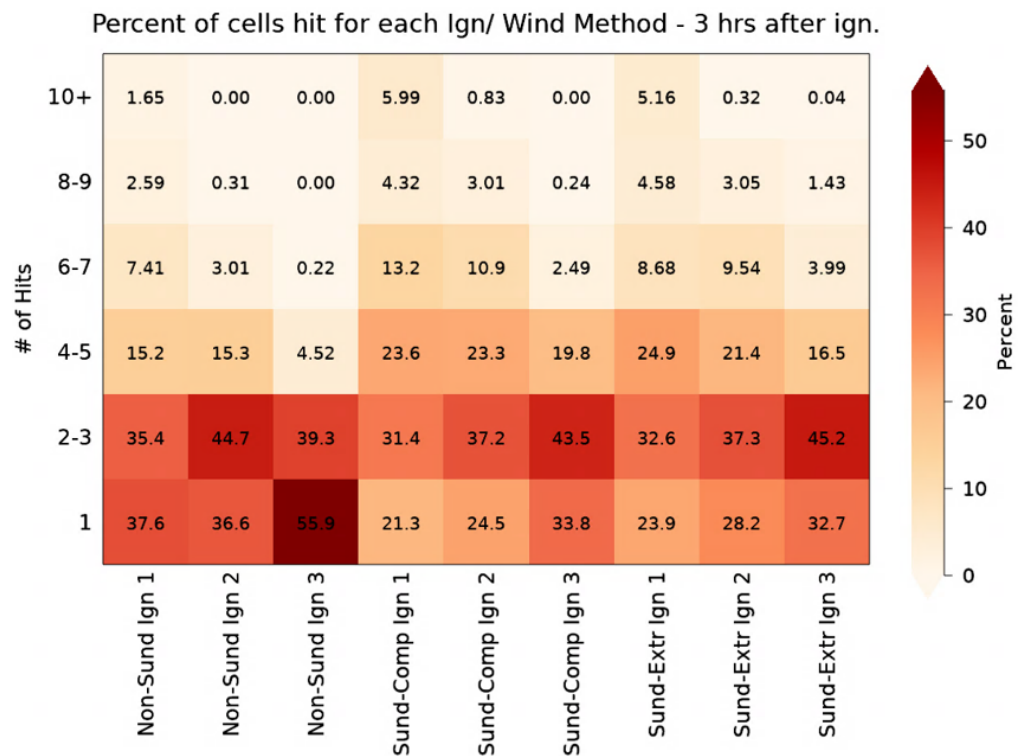


Figure 8. The percent of grid cells hit out for each “# of Hits” range considering the total number of grid cells hit for a particular ignition method/wind scenario combination.

3.2.2. Mean Sundowner Conditions

The composite of winds during Sundowners shows strong (~13 m/s) northerly winds present on the southern SYM slopes and in the foothills above Santa Barbara and Montecito (Figure 3b). For all ignition methods, the simulated wildfires grew larger than when the climatological winds were used (Figures 7 and 9) as a result of more southerly spread. In the runs using ignition method 1, the area around HWY 154 is hit more than 10 times for approximately 6% of the entire area burned (Figures 8 and 9). Although the middle of the subset area on the SYM slopes was not hit, there were two other clusters in the eastern part that were hit over eight times (Figure 9a). For simulations run using ignition methods 2 and 3, there were some area that were hit over eight times, but generally the fires were more spread out, resulting in a larger area of the entire region of interest hit in at least one simulation. Additionally, the east-west running Cathedral Oaks Road was hit by one simulation for ignition method 3, and multiple fires reached relatively close in all ignition modeling methods.

Similar to simulations run using the climatological winds, locations near HWY 154 were hit by the most simulations, up to 30 times when considering all ignition methods (Figure 6b). One differentiation from the climatological simulations is that an additional region of high risk is evident east of HWY 154. This implies that stronger winds spread fires further south than when weak winds were present. Furthermore, simulated fires spread more south toward the WUI and highly populated areas. In fact, most of the fires that reached the WUI slowed significantly around 2 h after ignition (green in Figure 9b,d,f). This may be due to the fuel model used in the WUI, which is difficult to burn and will slow or stop the fire in the model. It is important to note that FARSITE is generalizing the WUI materials and fuels, and thus these results indicate this region may be at higher risk, but that cannot be proven given the fuel and model limitations.

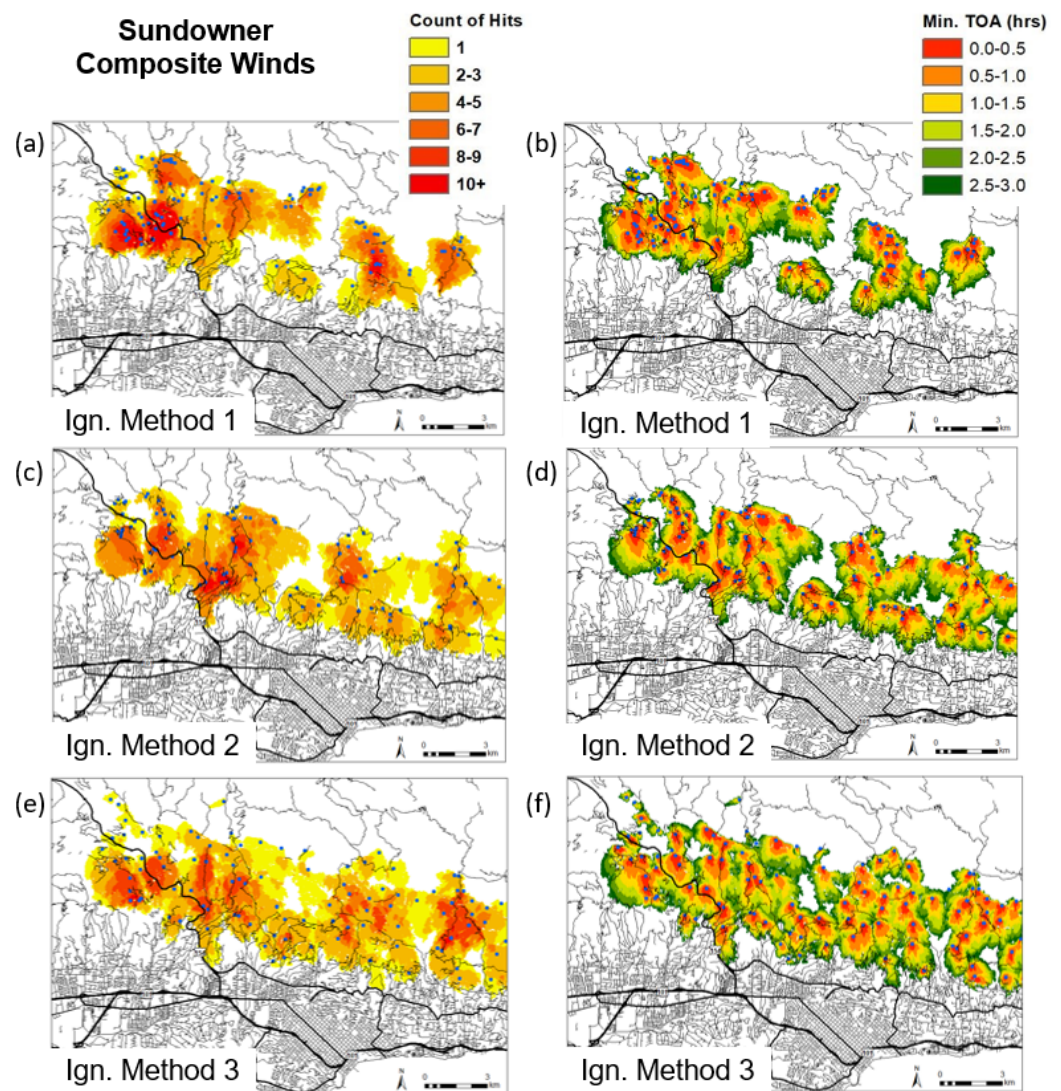


Figure 9. Same as Figure 5, but with wildfire simulations using the Sundowner composite winds. Maps (a) and (b) show results from ignition method 1, (c) and (d) show results from ignition method 2, and (e) and (f) show results from ignition method 3.

Overall, most simulated fires that used the Sundowner composite grew larger than those run using the climatological winds (Figure 7), which is expected since strong winds propagated the fires further southward. By 1 h after ignition, the mean and median fire size were around 30 ha, which grew to over 100 ha by 2 h after ignition, and the largest fires were around 500 ha only 3 h after ignition (Figure 7f). Interestingly, the majority of grid cells burned were hit 2–3 times regardless of ignition method, and ignition method 3 had over 75% of burned grid cells hit 1–3 times and none hit over 9 times (Figure 8).

3.2.3. Extreme Sundowner Winds: 14 April 2005 case study

During the extreme Sundowner case study, northeasterly winds exceeding 20 m/s were present across the southern SYM slopes and over the coastal cities (Figure 3c). These strong winds rapidly spread the simulated wildfires southwest toward urban areas (Figure 10). Similar to the previous runs using ignition method 1, HWY 154 was a hot spot for wildfire activity since many ignitions were nearby, and there was an area in the east that was hit many times as well. Cathedral Oaks Road, which is a significant evacuation route for many communities in the WUI, was reached by five simulations in ignition method 1 (Figure 10a), and these fires spread quickly into the city, particularly within the first 1.5 h

(red, orange, and yellow in Figure 10b). For ignition methods 2 and 3, the majority of the southern SYM slopes was hit in at least one simulation (Figure 10c,e). For ignition method 2, Cathedral Oaks Road was hit by five simulations, and it was hit by over 10 simulations in ignition method 3, in part due to the closer proximity of ignition points to urban areas. It is important to note that with ignition method 3, two simulations reached Cathedral Oaks Road within half an hour after ignition (Figure 10f). This implies that during Sundowners with strong winds over the WUI, wildfires ignited in the foothills near the city may reach urban areas exceptionally fast, and it may be best to have firefighting crews and resources ready to act.

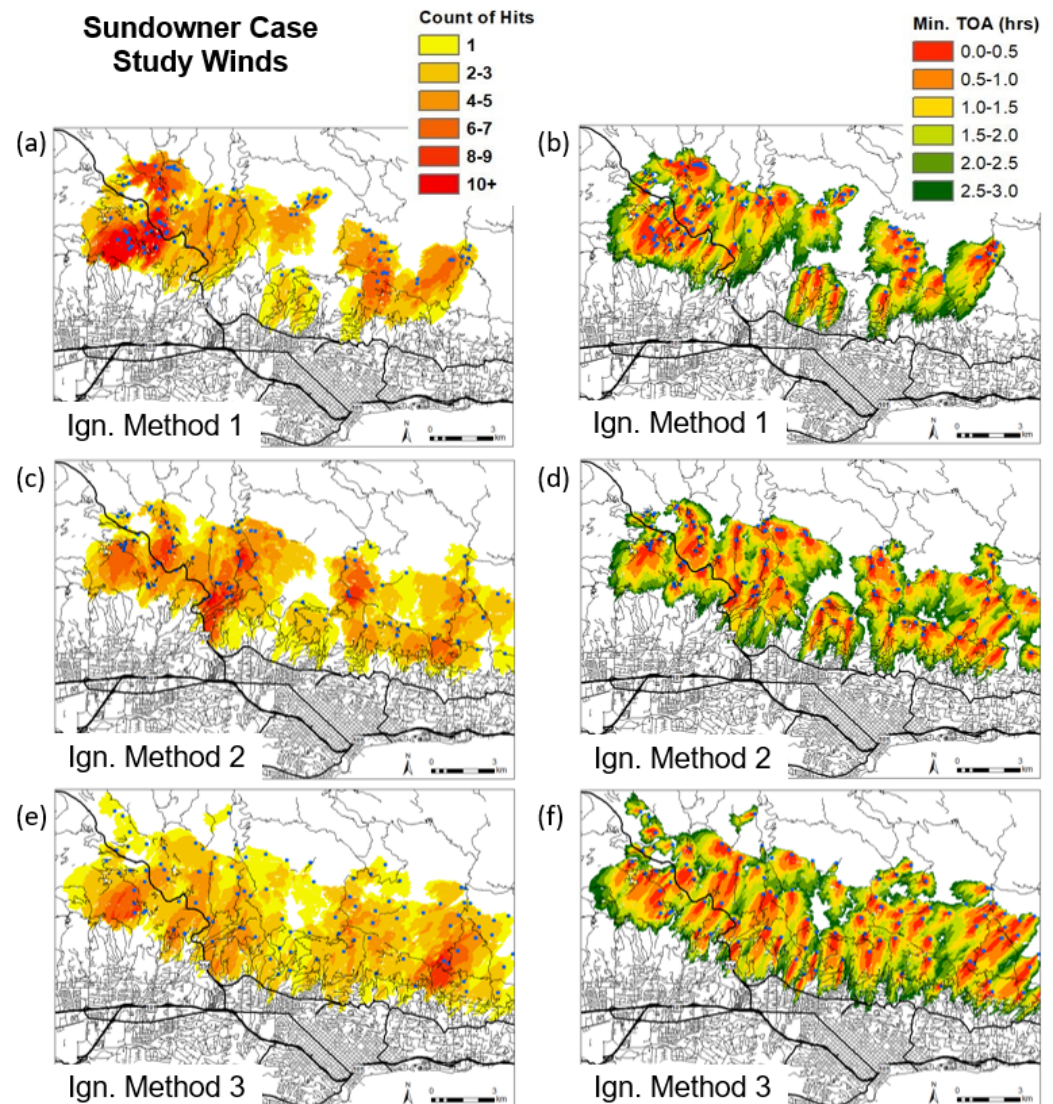


Figure 10. Same as Figure 5, but with wildfire simulations using the extreme Sundowner winds. Maps (a) and (b) show results from ignition method 1, (c) and (d) show results from ignition method 2, and (e) and (f) show results from ignition method 3.

When all ignition methods are combined and extreme Sundowner winds are used, over 10% of simulations (31 hits) occur near HWY 154 (Figure 6c). The use of these strong winds led to the simulated wildfires reaching more areas in the domain than when other wind scenarios were used, explained by the strong winds spreading fires further south. Additionally, the east part of the region exhibits areas where over 13 simulations hit (~4% of the total amount of simulations), and these areas are larger and further south than in the other wind scenarios. Perhaps the most important feature to note is that a large portion of

both HWY 154 and Cathedral Oaks Road were hit by at least 1 simulation when extreme winds were used (Figure 6c). Recall that spotting was disabled for these runs due to limitations found in [30], and historical wildfires such as the 1990 Painted Cave fire spread rapidly into urban areas driven by downstream spotting. Therefore, these simulations are likely underestimating how rapidly a fire may spread southward. A more sophisticated fire and ember model would be required to adequately identify the potential effects of spotting.

The size of wildfires simulated using extreme Sundowner winds were comparable to those from the Sundowner composite simulations (Figure 7), but the largest fires were produced from the Sundowner case study wind simulations. Similar to the Sundowner composite simulations, the majority of cells burned were hit by 1–3 simulations (Figure 8). Notice that the simulations using ignition method 1 for this extreme case resulted in the largest number of cells hit by wildfires. Overall, all ignition methods hit HWY 154 repeatedly and the Sundowner composite and Sundowner case study winds spread fires more rapidly to the south toward populated areas, with some reaching Cathedral Oaks Road.

3.2.4. Analysis of All Simulations

Figure 11 shows the count of hits for all 900 simulations, regardless of ignition method and wind scenario. Nearly all grid cells on the entire SYM slopes were hit in at least one simulation, and a few areas stand out as higher wildfire risk according to our simulations. On the SYM slopes to the west of HWY 154 and north of the city of Goleta, some grid cells were hit by 80 simulations, or 8.9% of the total simulations run. Slightly to the east of this maximum, over 50 simulations hit the regions directly next to the major route HWY 154, the main road running north from coastal Santa Barbara. This region has been hit by a handful of wildfires in the past, including the 1990 Painted Cave, 2009 Jesusita, and 2020 Cave fires, making this a high-risk area for wildfires.

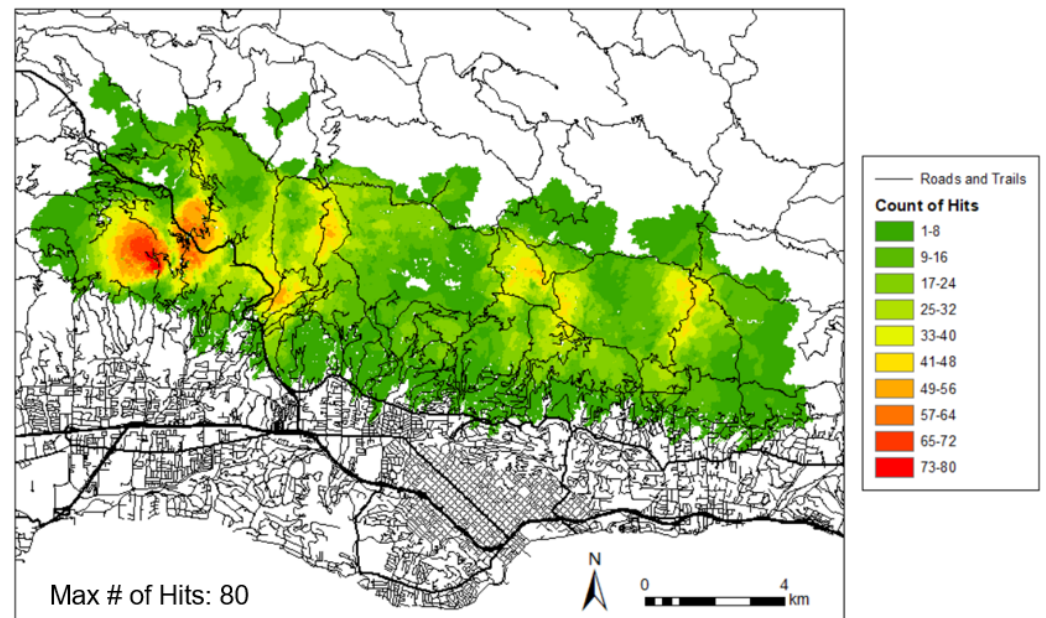


Figure 11. Similar to Figure 6, but using all simulations, regardless of ignition modeling method and wind scenario input.

Other grid cells in areas to the east (on the SYM slopes overlooking Santa Barbara and Montecito) have clusters with over 40 simulation hits (yellow in Figure 11). This is mainly around roads and trails, where the number of ignitions is higher based on the ignition modeling methods. Finally, similar to the results from the simulations run using the extreme Sundowner wind scenario, a large portion of Cathedral Oaks Road was hit by at least one simulation. Many people depend on this road daily, as it is the only entrance and exit to some homes and businesses on the mountain slopes. The fact that it was hit

in multiple locations highlights the importance of increasing wildfire resilience through understanding high-risk regions and improving firefighting and evacuation strategies.

4. Discussion and Conclusions

With an increasing trend of communities living in the WUI and roads and trails built further into the wilderness, identifying regions at high ignition risk is the first step toward improving wildfire prevention and enhancing strategies to protect the community. This is particularly imperative during critical fire weather conditions such as Sundowner wind events. This study examined wildfire risk in the Santa Barbara WUI on the south-facing slopes of the Santa Ynez Mountains. This region, located in southern California, has experienced numerous wildfires that rapidly spread toward populated areas to the south, driven by strong Sundowner winds. Although impactful wildfires have affected the whole extent of the southern SYM slopes, for computation reasons this study focuses on a domain north of the cities of Santa Barbara and Montecito, where the community is bounded by the mountains and the coast (Figure 1).

Observational datasets from the last few decades show a pattern of ignitions strongly linked to the proximity from roads and trails, clearly suggesting an anthropogenic connection with wildfires in the region. However, the observed ignitions were not uniformly distributed throughout the area of interest on the southern SYM slopes. For instance, the density of ignitions is higher in the western part near the main north–south route, HWY 154, and more generally around roads near the mountain ridge. Nonetheless, although the pattern of ignitions may be linked to the density of homes in the WUI, road traffic, and trails in this region, the persistent drought conditions and other unforeseen natural and/or anthropogenic changes may increase ignition probability in other regions that had previously observed relatively few ignitions. To account for these possible additional scenarios, we propose three ignition modeling methods and three distinct wind scenarios to investigate fire risk in this region, maintaining other meteorological variables, which are related to live fuel moisture, reflective of the extreme conditions from the 1990 Painted Cave fire.

The majority of ignition modeling studies have examined the relationship between observed ignitions and other variables such as human development and infrastructure [7,8,16–18,21]. Previous simulation studies have utilized a single ignition modeling method [47,53] or relied on previous ignitions [54] for runs. Furthermore, almost all previous research on ignitions and simulations in southern California is focused in a different area, such as the Santa Monica Mountains [18,47]. This novel study analyzed a new location highly impacted by wildfires, coastal Santa Barbara, and compared various ignition modeling methods and the resulting simulations.

Modeled ignitions were created in ignition method 1 by randomly sampling from buffers up to 500 m from previous ignition locations. This had the most clustered ignition points, with an absence of ignitions in the middle part of the area of interest due to a lack of previously observed ignitions. A large amount of the modeled ignitions was in the western part of the domain near HWY 154 (Figure 2a), which is a major road and evacuation route running north–south from the city. Regardless of the wind scenario, the area by HWY 154 was continuously hit the most in simulations due to the higher density of ignition points in this region (Figures 5, 9 and 10).

When ignitions were randomly sampled from a 50 m buffer around all roads and trails on the south SYM slopes (Figure 2b), similar to a methodology used in [47], the ignitions were more spread out, though gaps were still evident where no roads or trails are present. Similar to ignition method 1, the regions with the most simulation hits were near HWY 154 and in a few regions in the eastern part. More ignitions were closer to the WUI and urban areas in the south, thus more simulations spread into the WUI closer to the coastal communities in Santa Barbara.

When ignitions were sampled using a distance decay function around roads and trails up to 1000 m with the probability of ignition selection linearly decreasing with increasing distance from the road or trail (Figure 2c), the spatial distribution of ignitions was the most

expansive in the area of interest because ignitions were not restricted by a harsh buffer around previous ignitions or roads and trails; the ignitions were the furthest north and south points out of all methods (Figure A3). There were very few grid cells that were not hit by any simulations on the mountain slopes (Figures 5, 9 and 10). Furthermore, many fires reached Cathedral Oaks Road, and some simulations spread south of the road as well (Figure 10).

In addition to the different ignition methods, varying the wind scenario greatly changed the shape and size of the simulations, and varied the regions that were considered at risk, especially in the WUI. During climatological conditions, the simulated fires did not travel far from the ignition source and spread in a radial pattern (Figure 5), resulting in the smallest fires of all wind methods (Figure 7). This indicates that during climatological conditions, wildfires may be less likely to spread rapidly and less likely to cause large, destructive wildfires in this region. Fires spread further south and grew larger when the Sundowner composite and extreme Sundowner case study winds were used in the simulations. For the Sundowner composite and Sundowner case study conditions, simulated wildfires reached heavily trafficked areas due to the strong north and northeasterly winds (Figure 6b,c). When the Sundowner case study winds were used with ignition method 3, some simulations reached Cathedral Oaks Road and the surrounding WUI within the first half an hour (Figure 10f).

Limitations are inherent in this work. Wildfires ignited via powerlines were not considered in this work, though they were found as a major ignition source in [11]. As explained in the introduction, FARSITE does not model spotting when fires spread downslope and thus was disabled in our simulations. It is known that spotting can be an important factor in the rapid spread of wildfires [30], so the maps produced in this study are likely more conservative. A different model with more computational expenses would be required to model how enabling spotting would influence fire risk in this region. Furthermore, the fuel map used in simulations had no burn scars (Figure A2) and the live fuel moisture values used were the lowest possible observed for the vegetation in this region. The lack of burn scars may highlight regions as high risk when a recent fire in that location may lessen the potential risk. Thus, these findings must be taken with consideration to recent events and fuel moisture at that time. As far as the wind scenarios, by their nature, composites may smooth out more extreme conditions, as shown by the differences in winds between the Sundowner composite wind raster and the Sundowner case study raster (Figure 3b,c). Although we only looked at simulations for one extreme Sundowner case study, each Sundowner has individual characteristics and spatial extents. Additionally, these results were analyzed for only 3 h after ignition, and expanding the simulation time may highlight other areas where an ignition may threaten this area.

Future work may include creating additional ignition points in this region, potentially expanding into the valley to the north or considering other ignition sources such as powerlines and running simulations to more thoroughly cover the southern SYM slope. Other extreme case studies may be used as wind scenarios and input in FARSITE to highlight areas more accurately at highest risk during extreme fire weather. Another idea is to examine the ability to identify a region of potential ignition locations for a specific point by reversing topography and winds. It may be beneficial to understand whether an ignition at a given location is probable to impact a specific point on a major evacuation route, such as HWY 154 or Cathedral Oaks Road. Nevertheless, the findings from this study may assist wildfire planners and city officials by providing guidance for resource and staffing allocations on days with weak to strong winds. In addition, this may help focus locations for improvements in evacuation planning, road and trail design, creation of defensive space around properties and transmission lines, and other public policies to prevent and mitigate the effects of wildfires.

Author Contributions: Conceptualization, K.Z., L.M.V.C., C.J., G.-J.D., D.R., F.F., M.M., N.E. and R.H.; methodology, K.Z., L.M.V.C., C.J., J.B., G.-J.D., D.R., F.F. and M.M.; software, K.Z. and J.B.; formal analysis, K.Z.; data curation, K.Z. and C.J.; writing—original draft preparation, K.Z.; writing—review and editing, K.Z., L.M.V.C., C.J., J.B., G.-J.D., D.R., F.F., M.M., N.E. and R.H.; visualization, K.Z.; supervision, L.M.V.C.; project administration, K.Z. and L.M.V.C.; funding acquisition, L.M.V.C., C.J., D.R. and M.M. All authors have read and agreed to the published version of the manuscript.

Funding: This research was supported by the National Science Foundation: PREEVENTS ICER—1664173; National Science Foundation: Physical and Dynamic Meteorology program (NSF-1921595); University of California Office of the President Laboratory Fees Program (LFR-20-652467).

Informed Consent Statement: Not applicable.

Acknowledgments: This research was completed with the help of the Montecito, Santa Barbara, and Santa Barbara County Fire Departments and the National Weather Service—Los Angeles/Oxnard Office.

Conflicts of Interest: The authors declare no conflict of interest.

Appendix A

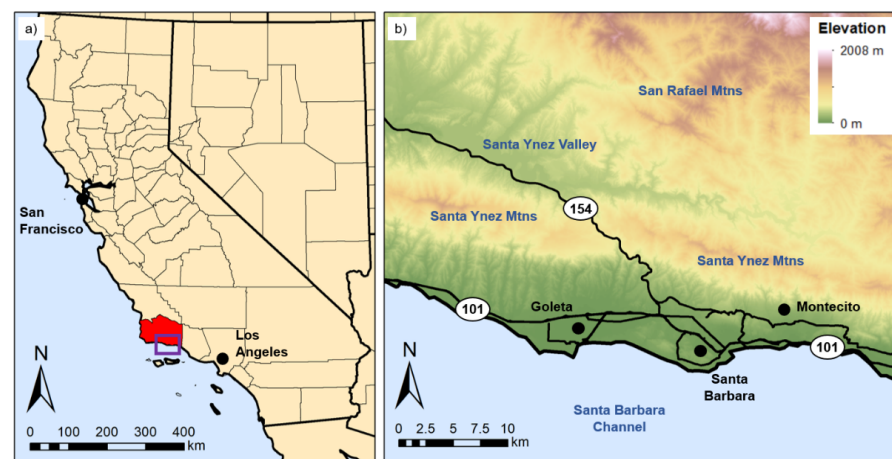


Figure A1. (a) State and county borders, with Santa Barbara County colored red. (b) Topography in southern Santa Barbara County (see purple box in (a) for subset). Cities are in black text and geographic features are in blue text. The thick lines indicate major roads, and highways are labeled.

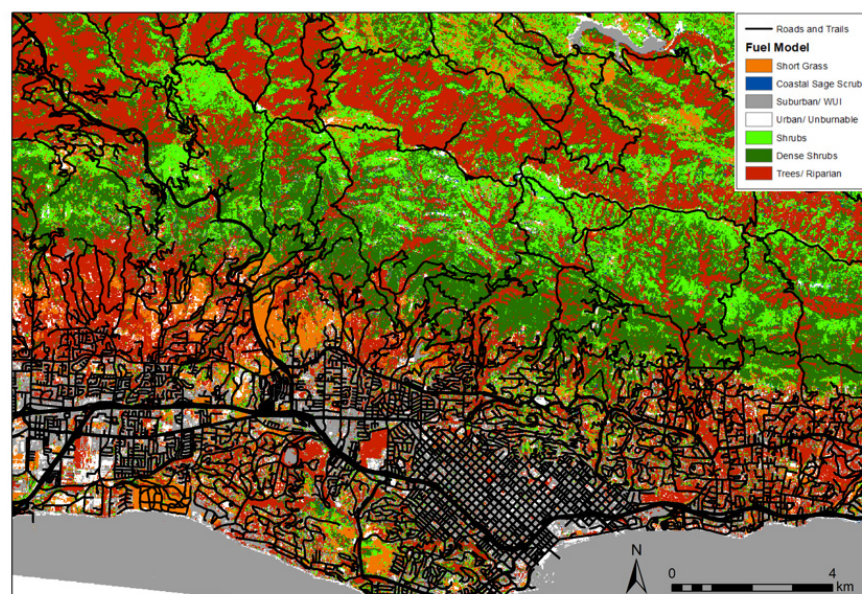


Figure A2. Fuel map for the wildfire simulations. Fuel model information can be found in [30].

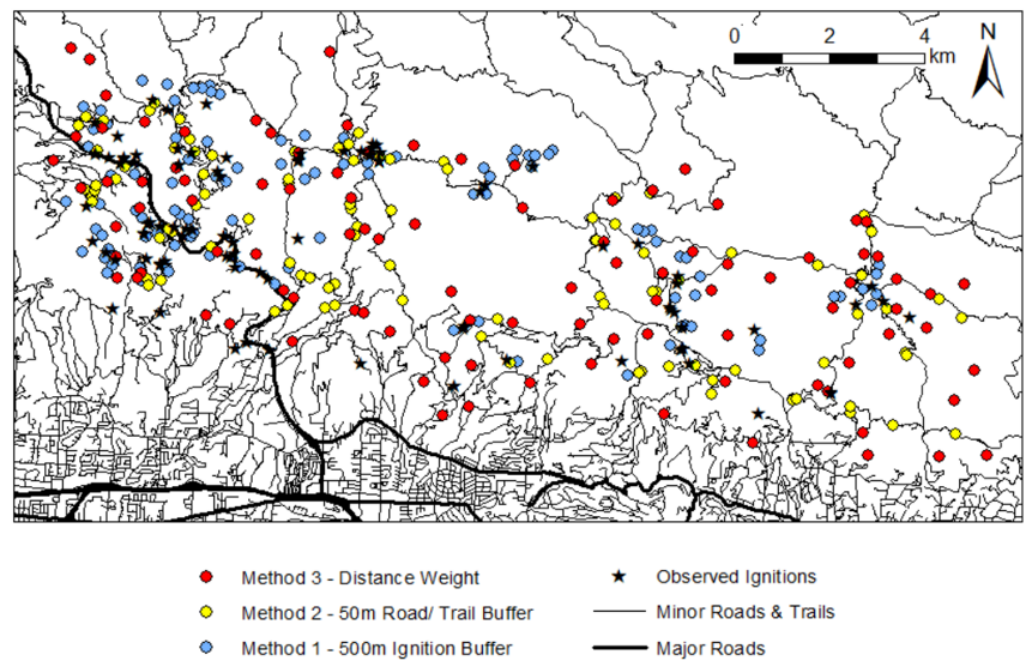


Figure A3. Ignition points from the three ignition modeling methods (colored dots) and previous ignition locations (black stars) overlaid on roads and trails (black lines).

References

1. Radeloff, V.C.; Hammer, R.B.; Stewart, S.I.; Fried, J.S.; Holcomb, S.S.; McKeefry, J.F. The wildland–urban interface in the United States. *Ecol. appl.* **2005**, *15*, 799–805. [[CrossRef](#)]
2. Radeloff, V.C.; Helmers, D.P.; Kramer, H.A.; Mockrin, M.H.; Alexandre, P.M.; Bar-Massada, A.; Butsic, V.; Hawbaker, T.J.; Martinuzzi, S.; Syphard, A.D.; et al. Rapid growth of the US wildland-urban interface raises wildfire risk. *Proc. Natl. Acad. Sci. USA* **2018**, *115*, 3314–3319. [[CrossRef](#)] [[PubMed](#)]
3. Hammer, R.B.; Stewart, S.I.; Radeloff, V.C. Demographic trends, the wildland–urban interface, and wildfire management. *Soc. Nat. Resour.* **2009**, *22*, 777–782. [[CrossRef](#)]
4. Moritz, M.A.; Batllori, E.; Bradstock, R.A.; Gill, A.M.; Handmer, J.; Hessburg, P.F.; Leonard, J.; McCaffrey, S.; Odion, D.C.; Schoennagel, T.; et al. Learning to coexist with wildfire. *Nature* **2014**, *515*, 58–66. [[CrossRef](#)]
5. Kramer, H.A.; Mockrin, M.H.; Alexandre, P.M.; Radeloff, V.C. High wildfire damage in interface communities in California. *Int. J. Wildland Fire* **2019**, *28*, 641–650. [[CrossRef](#)]
6. Keeley, J.E.; Fotheringham, C.J.; Moritz, M.A. Lessons from the October 2003 Wildfires in Southern California. *J. For.* **2004**, *102*, 26–31.
7. Syphard, A.D.; Radeloff, V.C.; Keeley, J.E.; Hawbaker, T.J.; Clayton, M.K.; Stewart, S.I.; Hammer, R.B. Human influence on California fire regimes. *Ecol. Appl.* **2007**, *17*, 1388–1402. [[CrossRef](#)]
8. Faivre, N.; Jin, Y.; Goulden, M.L.; Randerson, J.T. Controls on the spatial pattern of wildfire ignitions in Southern California. *Int. J. Wildland Fire* **2014**, *23*, 799–811. [[CrossRef](#)]
9. Bryant, B.P.; Westerling, A.L. Scenarios for future wildfire risk in California: Links between changing demography, land use, climate, and wildfire. *Environmetrics* **2014**, *25*, 454–471. [[CrossRef](#)]
10. Balch, J.K.; Bradley, B.A.; Abatzoglou, J.T.; Nagy, R.C.; Fusco, E.J.; Mahood, A.L. Human-started wildfires expand the fire niche across the United States. *Proc. Natl. Acad. Sci. USA* **2017**, *114*, 2946–2951. [[CrossRef](#)]
11. Keeley, J.E.; Syphard, A.D. Historical patterns of wildfire ignition sources in California ecosystems. *Int. J. Wildland Fire* **2018**, *27*, 781–799. [[CrossRef](#)]
12. Moritz, M.A.; Knowles, S.G. Coexisting with wildfire. *Am. Sci.* **2016**, *104*, 220.
13. Nauslar, N.J.; Abatzoglou, J.T.; Marsh, P.T. The 2017 North Bay and Southern California fires: A case study. *Fire* **2018**, *1*, 18. [[CrossRef](#)]
14. Bartlein, P.J.; Hostetler, S.W.; Shafer, S.L.; Holman, J.O.; Solomon, A.M. Temporal and spatial structure in a daily wildfire-start data set from the western United States (1986–1996). *Int. J. Wildland Fire* **2008**, *17*, 8–17. [[CrossRef](#)]
15. Jin, Y.; Randerson, J.T.; Faivre, N.; Capps, S.; Hall, A.; Goulden, M.L. Contrasting controls on wildland fires in Southern California during periods with and without Santa Ana winds. *J. Geophys. Res. Biogeosciences* **2014**, *119*, 432–450. [[CrossRef](#)]
16. Syphard, A.D.; Radeloff, V.C.; Keuler, N.S.; Taylor, R.S.; Hawbaker, T.J.; Stewart, S.I.; Clayton, M.K. Predicting spatial patterns of fire on a southern California landscape. *Int. J. Wildland Fire* **2008**, *17*, 602–613. [[CrossRef](#)]

17. Syphard, A.D.; Keeley, J.E.; Massada, A.B.; Brennan, T.J.; Radeloff, V.C. Housing arrangement and location determine the likelihood of housing loss due to wildfire. *PLoS ONE* **2012**, *7*, e33954. [[CrossRef](#)]
18. Syphard, A.D.; Keeley, J.E. Location, timing and extent of wildfire vary by cause of ignition. *Int. J. Wildland Fire* **2015**, *24*, 37–47. [[CrossRef](#)]
19. Countryman, C.M. *The Fire Environment Concept*; USDA Forest Service: Berkeley, CA, USA, 1972; p. 15.
20. Moritz, M.A. Spatiotemporal analysis of controls on shrubland fire regimes: Age dependency and fire hazard. *Ecology* **2003**, *84*, 351–361. [[CrossRef](#)]
21. Abatzoglou, J.T.; Balch, J.K.; Bradley, B.A.; Kolden, C.A. Human-related ignitions concurrent with high winds promote large wildfires across the USA. *Int. J. Wildland Fire* **2018**, *27*, 377–386. [[CrossRef](#)]
22. Blier, W. The sundowner winds of Santa Barbara, California. *Weather. Forecast.* **1998**, *13*, 702–716. [[CrossRef](#)]
23. Jones, C.; Carvalho, L.; Duine, G.J.; Zigner, K. A New Climatology of Sundowner Winds in Coastal Santa Barbara, California, Based on 30-yr High Resolution WRF Downscaling. *Atmos. Res.* **2021**, *249*, 105305. [[CrossRef](#)]
24. Zigner, K.; Carvalho, L.; Jones, C.; Duine, G.J. Extreme winds and fire weather in coastal Santa Barbara County, CA: An observational analysis. *Int. J. Clim.* **2021**, *41*, 597–618. [[CrossRef](#)]
25. Cannon, F.; Carvalho, L.; Jones, C.; Hall, T.; Gomberg, D.; Dumas, J.; Jackson, M. WRF Simulation of Downslope Wind Events in Coastal Santa Barbara County. *Atmos. Res.* **2017**, *191*, 57–73. [[CrossRef](#)]
26. Carvalho, L.; Duine, G.J.; Jones, C.; Zigner, K.; Clements, C.; Kane, H.; Gore, G.; Bell, G.; Gamelin, B.; Gomberg, D.; et al. The Sundowner Winds Experiment (SWEX) Pilot Study: Understanding Downslope Windstorms in the Santa Ynez Mountains, Santa Barbara, CA. *Mon. Weather. Rev.* **2020**, *148*, 1519–1539. [[CrossRef](#)]
27. Duine, G.J.; Jones, C.; Carvalho, L.M.V.; Fovell, R.G. Simulating Sundowner Winds in Coastal Santa Barbara: Model Validation and Sensitivity. *Atmosphere* **2019**, *10*, 155. [[CrossRef](#)]
28. Duine, G.J.; Carvalho, L.M.; Jones, C.; Zigner, K. The effect of upstream orography on the onset of sundowner winds in coastal Santa Barbara, CA. *J. Geophys. Res. Atmos.* **2021**, *126*, e2020JD033791. [[CrossRef](#)]
29. Duine, G.J.; Carvalho, L.M.V.; Jones, C. Mesoscale patterns associated with two distinct heatwave events in coastal Santa Barbara, California, and their impact on local fire risk conditions. *Weather. Clim. Extrem.* **2022**, *37*, 100482. [[CrossRef](#)]
30. Zigner, K.; Carvalho, L.; Peterson, S.; Fujioka, F.; Duine, G.J.; Jones, C.; Roberts, D.; Moritz, M. Evaluating the Ability of FARSITE to Simulate Wildfires Influenced by Extreme, Downslope Winds in Santa Barbara, California. *Fire* **2020**, *3*, 29. [[CrossRef](#)]
31. Kolden, C.A.; Abatzoglou, J.T. Spatial distribution of wildfires ignited under katabatic versus non-katabatic winds in mediterranean Southern California USA. *Fire* **2018**, *1*, 19. [[CrossRef](#)]
32. Skamarock, W.C.; Klemp, J.B.; Dudhia, J.; Gill, D.O.; Barker, D.M.; Wang, W.; Powers, J.G. A description of the Advanced Research WRF version 3. NCAR Technical note-475+ STR. *Univ. Corp. Atmos. Res.* **2008**.
33. Thompson, M.P.; Bowden, P.; Brough, A.; Scott, J.H.; Gilbertson-Day, J.; Taylor, A.; Anderson, J.; Haas, J.R. Application of wildfire risk assessment results to wildfire response planning in the southern Sierra Nevada, California, USA. *Forests* **2016**, *7*, 64. [[CrossRef](#)]
34. Keane, R.E.; Agee, J.K.; Fule, P.; Keeley, J.E.; Key, C.; Kitchen, S.G.; Schulte, L.A. Ecological effects of large fires on US landscapes: Benefit or catastrophe? *A. Int. J. Wildland Fire* **2009**, *17*, 696–712. [[CrossRef](#)]
35. Calkin, D.E.; Cohen, J.D.; Finney, M.A.; Thompson, M.P. How risk management can prevent future wildfire disasters in the wildland-urban interface. *Proc. Natl. Acad. Sci. USA* **2014**, *111*, 746–751. [[CrossRef](#)] [[PubMed](#)]
36. Arno, S.F.; Brown, J.K. *Overcoming the Paradox in Managing Wildland Fire*; Western Wildlands, Montana Forest and Conservation Experiment Station: Missoula, MT, USA, 1991; pp. 40–46.
37. Cohen, J. The wildland-urban interface fire problem. *Fremontia* **2010**, *38*, 16–22.
38. Syphard, A.D.; Brennan, T.J.; Keeley, J.E. The importance of building construction materials relative to other factors affecting structure survival during wildfire. *Int. J. Disaster Risk Reduction* **2017**, *21*, 140–147. [[CrossRef](#)]
39. Syphard, A.D.; Keeley, J.E. Factors associated with structure loss in the 2013–2018 California wildfires. *Fire* **2019**, *2*, 49. [[CrossRef](#)]
40. Finney, M.A. *FARSITE: Fire Area Simulator-Model Development and Evaluation*; U.S. Department of Agriculture, Forest Service, Rocky Mountain Research Station: Fort Collins, CO, USA, 1998.
41. Stratton, R.D. *Guidance on Spatial Wildland Fire Analysis: Models, Tools, and Techniques*; U.S. Department of Agriculture, Forest Service, Rocky Mountain Research Station: Ft. Collins, CO, USA, 2006.
42. Scott, J.H. *Comparison of Crown Fire Modeling Systems Used in Three Fire Management Applications*; U.S. Department of Agriculture, Forest Service, Rocky Mountain Research Station: Ft. Collins, CO, USA, 2006.
43. Finney, M.A.; Ryan, K.C. Use of the FARSITE Fire Growth Model for Fire Prediction in U.S. National Parks. In Proceedings of the International Emergency Management and Engineering Conference, San Diego, CA, USA, 9–12 May 1995; pp. 183–189.
44. Papadopoulos, G.D.; Pavlidou, F.N. A Comparative Review on Wildfire Simulators. *IEEE Syst. J.* **2011**, *5*, 233–243. [[CrossRef](#)]
45. Rothermel, R.C. *A Mathematical Model. for Predicting Fire Spread in Wildland Fuels*; U.S. Department of Agriculture, Forest Service, Intermountain Forest and Range Experiment Station: Ogden, UT, USA, 1972; p. 40.
46. Preisler, H.K.; Brillinger, D.R.; Burgan, R.E.; Benoit, J.W. Probability based models for estimation of wildfire risk. *Int. J. Wildland Fire* **2004**, *13*, 133–142. [[CrossRef](#)]
47. Peterson, S.H.; Moritz, M.A.; Morais, M.E.; Dennison, P.E.; Carlson, J.M. Modelling long-term fire regimes of southern California shrublands. *Int. J. Wildland Fire* **2011**, *20*, 1–16. [[CrossRef](#)]

48. Moritz, M.A.; Moody, T.J.; Krawchuk, M.A.; Hughes, M.; Hall, A. Spatial variation in extreme winds predicts large wildfire locations in chaparral ecosystems. *Geophys. Res. Lett.* **2010**, *37*. [[CrossRef](#)]
49. Parisien, M.A.; Snetsinger, S.; Greenberg, J.A.; Nelson, C.R.; Schoennagel, T.; Dobrowski, S.Z.; Moritz, M.A. Spatial variability in wildfire probability across the western United States. *Int. J. Wildland Fire* **2012**, *21*, 313–327. [[CrossRef](#)]
50. Murray, A.T.; Carvalho, L.; Church, R.L.; Jones, C.; Roberts, D.; Xu, J.; Zigner, K.; Nash, D. Coastal vulnerability under extreme weather. *Appl. Spat. Anal. Policy* **2020**, *14*, 1–27. [[CrossRef](#)]
51. Marsh, M. Santa Barbara County Fire Department, Santa Barbara, CA, USA. Personal communication, 2021.
52. Roth, K.L.; Dennison, P.E.; Roberts, D.A. Comparing Endmember Selection Techniques for Accurate Mapping of Plant Species and Land Cover Using Imaging Spectrometer Data. *Remote Sens. Environ.* **2012**, *127*, 139–152. [[CrossRef](#)]
53. Scott, J.H.; Thompson, M.P.; Calkin, D.E. *A Wildfire Risk Assessment Framework for Land and Resource Management*; RMRS-GTR-315; U.S. Department of Agriculture, Forest Service, Rocky Mountain Research Station: Ft. Collins, CO, USA, 2013.
54. Finney, M.A.; McHugh, C.W.; Grenfell, I.C.; Riley, K.L.; Short, K.C. A simulation of probabilistic wildfire risk components for the continental United States. *Stoch. Environ. Res. Risk Assess.* **2011**, *25*, 973–1000. [[CrossRef](#)]